

Supporting Information

Discovery and Structure-Based Optimization of Benzimidazole-Derived Activators of SOS1-Mediated Nucleotide Exchange on RAS

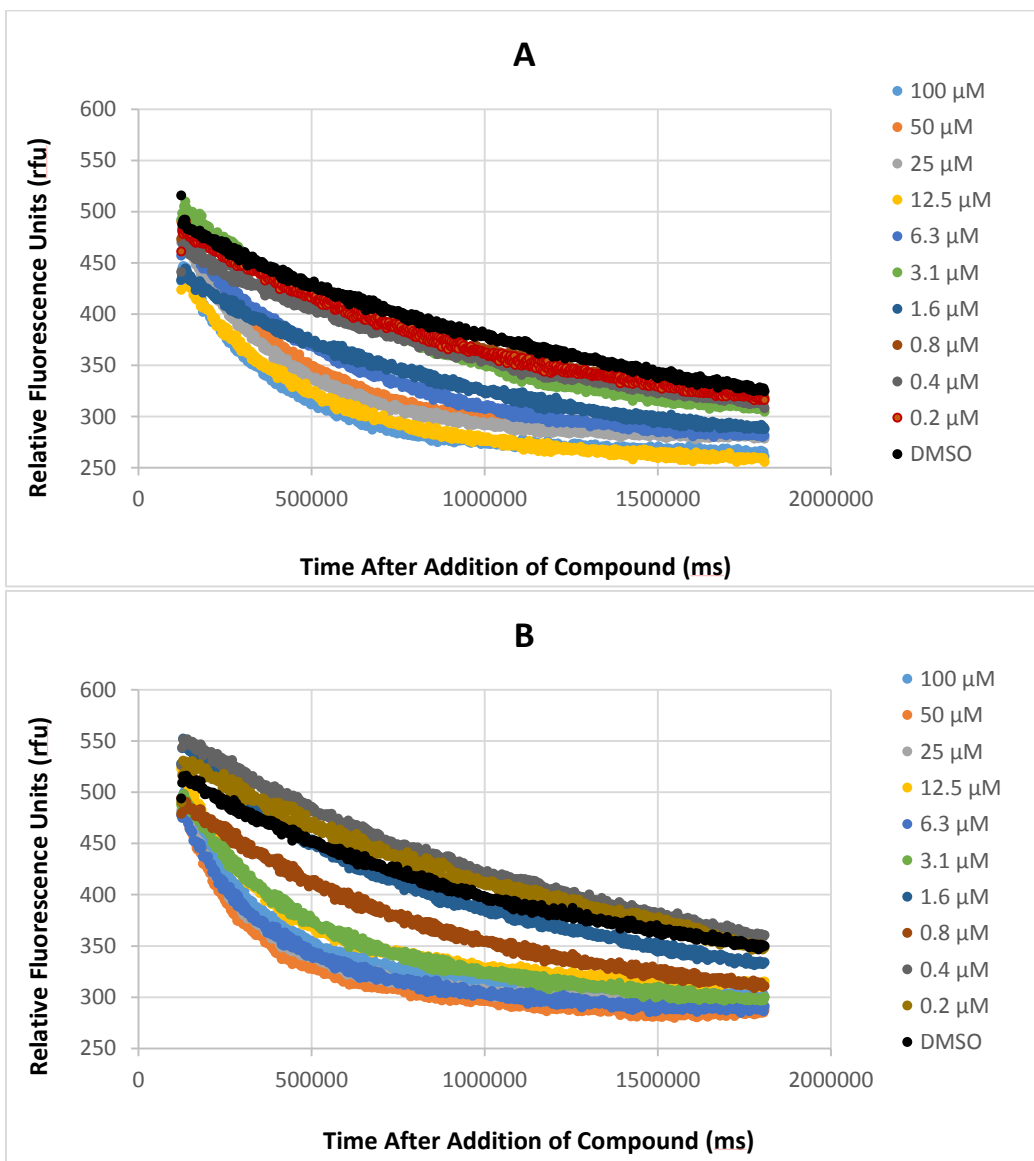
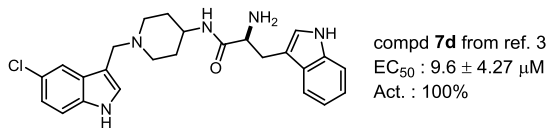
Timothy R. Hodges, Jason R. Abbott, Andrew J. Little, Dhruva Sarkar, James M. Salovich, Jennifer E. Howes, Denis T. Akan, Jiqing Sai, Allison L. Arnold, Carrie Browning, Michael C. Burns, Tammy Sobolik, Qi Sun, Yugandhar Beesetty, Jesse A. Coker, Dirk Scharn, Heinz Stadtmueller, Olivia W. Rossanese, Jason Phan, Alex G. Waterson, Darryl B. McConnell, and Stephen W. Fesik

Table of Contents

I.	<i>Biology Experimental Details</i>	S2
a.	Nucleotide Exchange Assay.	S2
i.	Figure S1. Representative Nucleotide Exchange Assays.	S2
b.	Fluorescence Polarization Competition Assays.	S3
c.	Fluorescence Polarization Saturation Binding Assay.	S3
i.	Figure S2. Saturation Binding Curves for S1 , S2 , and S3 .	S4
d.	Supplementary FPA and Nucleotide Exchange Data.	S5
i.	Figure S3. FPA vs Nucleotide Exchange.	S5
ii.	Table S1. Comparison of Nucleotide Exchange EC ₅₀ and FPA K _d .	S5
e.	Solubility and Permeability Measurements.	S6
i.	Table S2. In Vitro Solubility and Permeability Measurements for Select Compounds.	S6
f.	Cell Culture.	S7
g.	Active RAS-GTP Pull-Down and Western Blotting.	S7
h.	In-Cell Western.	S7
i.	Figure S4. In-Cell Western Analysis.	S8
II.	<i>Chemistry Experimental Details</i>	S9
a.	Syntheses of FPA Probes.	S9
i.	Scheme S1. Synthesis of FPA Probe S1 .	S9
ii.	Scheme S2. Synthesis of FPA Probe S2 .	S10
iii.	Scheme S3. Synthesis of FPA Probe S3 .	S11
III.	<i>Structural Biology Experimental Details</i>	S12
a.	Protein Expression and Purification.	S12
b.	Crystallization, X-ray Data Collection, Structure Solution, and Refinement.	S12
i.	Table S3. X-ray Data Collection and Refinement Statistics.	S12
IV.	<i>References</i>	S15

Biology Experimental Details

Nucleotide Exchange Assay. Nucleotide exchange assays were conducted as reported previously.¹⁻³ Compound **7d**, as reported in reference 3, was used as the reference compound for which Act. values were normalized to.



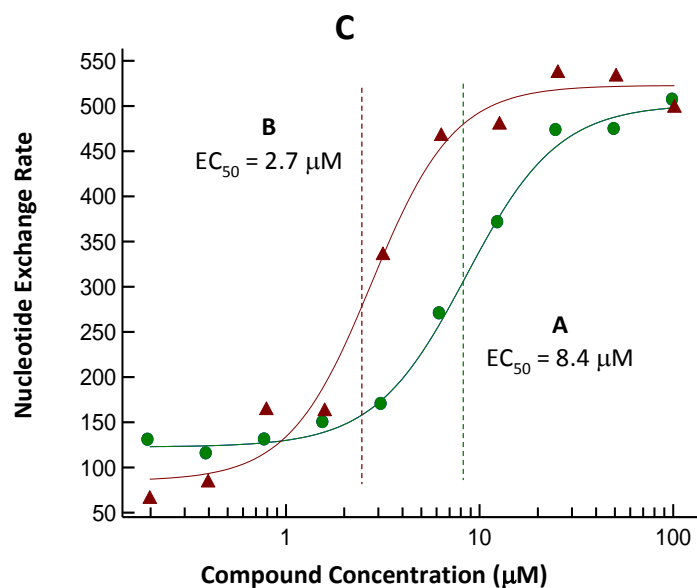


Figure S1. (A) Representative nucleotide exchange data from a single experiment and a single replicate for the indole control compound measuring the loss of relative fluorescence over time in the presence of varying concentrations of compound. (B) Nucleotide exchange data from a single experiment and a single replicate for a representative benzimidazole compound measuring the loss of relative fluorescence over time in the presence of varying concentrations of compound. (C) Representative EC₅₀ curves generated from the rates of nucleotide exchange generated from plots A and B vs. compound concentration. The green circles represent rate data calculated from plot A and the maroon triangles represent rate data calculated from plot B. The dotted vertical lines indicate how the EC₅₀ values of nucleotide exchange for the corresponding compounds were determined.

Fluorescence Polarization Competition Assays. Three different fluorescent probes were used in these assays: **S1**, **S2**, and **S3** (Figure S1). FPA measurements were carried out in 384-well, black, flat-bottom plates (Greiner 781900) using a Cytation 3 image reader (Biotek, Winooski, VT). All assays were conducted in assay buffer containing 20 mM Tris-HCl pH 7.5, 50 mM NaCl, 1 mM MgCl. Compounds were diluted in a 12-point, 3-fold serial dilution scheme and equal volumes of buffer to compound were added to all wells and mixed thoroughly. To an assay plate, 4 μL of diluted compound was added per well and then 56 μL of SOS1 protein (SOS^{cat}, amino acids 564–1049,⁴ at final concentration 156 nM for probes **S1** and **S2**, and 10 nM for probe **S3**) was added. The plate was left at room temperature for 20 min and then 20 μL of probe solution was added (final concentration was 50 nM for probes **S1** and **S2**, and 10 nM for **S3**), achieving a final DMSO concentration of 2.5% per well. After 20 min at room temperature in the absence of light, anisotropy was measured using a Cytation 3 image reader. IC₅₀ (inhibitor concentration at which 50% of bound peptide is displaced) was calculated by fitting the inhibition data using XLFit software (Guildford, UK) to a single-site binding model. This was converted into a binding dissociation constant (K_d) according to the formula⁵:

$$K_d = [I]_{50} / ([L]_{50} / K_d^{\text{probe}} + [P]_0 / K_d^{\text{probe}} + 1)$$

where $[I]_{50}$ is the concentration of the free inhibitor at 50% inhibition, $[L]_{50}$ is the concentration of the free labeled probe at 50% inhibition, $[P]_0$ is the concentration of the free protein at 0% inhibition, and K_d^{probe} represents the dissociation constant of the FITC-labeled probe derived from saturation binding experiments outlined below. Each compound was assessed at least twice independently, and in duplicate on each plate.

Fluorescence Polarization Saturation Binding Assay. Fluorescein-labeled small molecule probes **S1**, **S2**, and **S3** were titrated with the SOS1 protein (SOS^{cat}, amino acids 564–1049).⁴ FPA measurements were conducted under the same conditions as described above. To measure association of probe **S1** or **S2** to SOS1, 50 nM probe was incubated with varying concentrations of the SOS1 protein prepared using a 12-point, 2-fold serial dilution with the top concentration equaling 10 μM. To measure association of the **S3** probe to SOS1, 50 nM probe was incubated with

varying concentrations of the SOS1 protein prepared using a 16-point, 3-fold serial dilution with the top concentration equaling 10 μM .

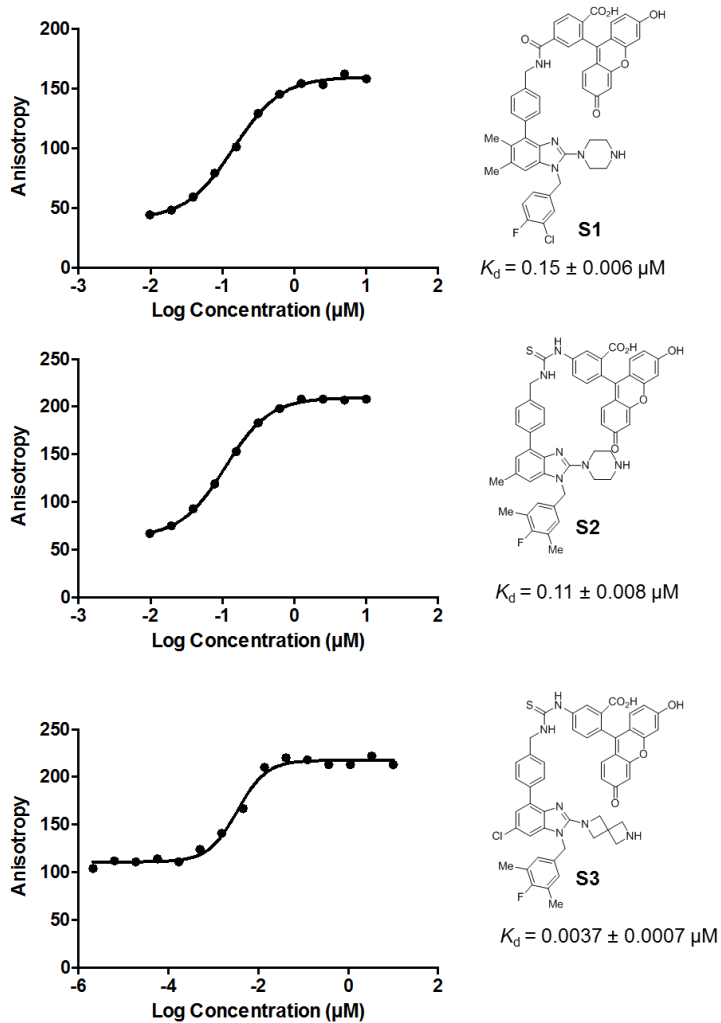


Figure S2. Saturation binding curves for FPA probes S1, S2, and S3. K_d measurements are reported as the mean \pm SD of at least three independent experiments.

Supplementary FPA and Nucleotide Exchange Data.

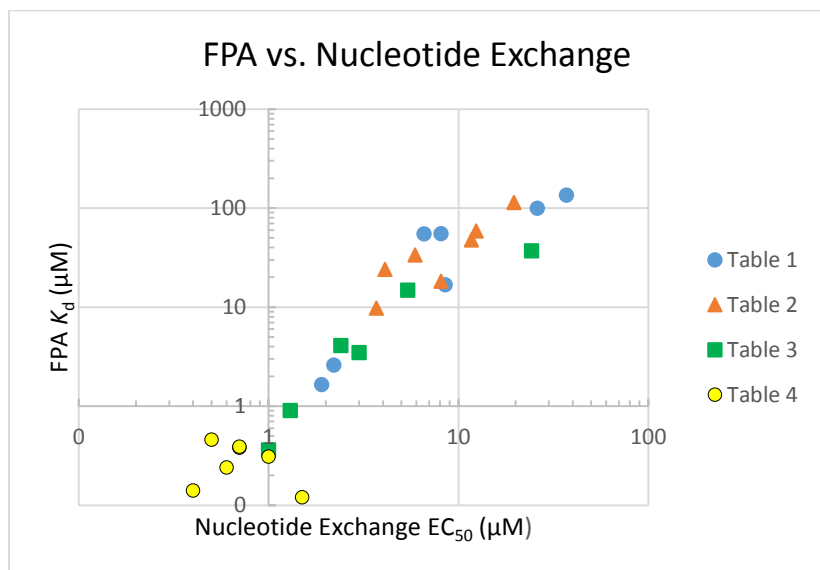


Figure S3. Correlation between FPA K_d and Nucleotide Exchange EC_{50} .

Table S1. Comparison of Nucleotide Exchange EC_{50} and FPA K_d .^a

Compd	EC_{50} (μM)	K_d (μM) ^b	Location
3	8.1	55.0 ^c	Table 1
5	37.1	134.4	Table 1
6	26.0	99.6	Table 1
7	8.5	16.8	Table 1
8	6.6	54.6	Table 1
10	2.2	2.59 ^c	Table 1
11	1.9	1.65	Table 1
14	12.4	58.8	Table 2
16	19.6	113.6	Table 2
17	5.9	33.6	Table 2
18	4.1	24.0	Table 2
19	8.1	18.3	Table 2
20	11.7	47.4	Table 2
21	3.7	9.73	Table 2
22	3.0	3.46	Table 3
23	5.4	14.8	Table 3
24	2.4	4.09	Table 3
26	24.3	36.9	Table 3
27	1.3	0.90	Table 3
28	1.0	0.36	Table 3
29	0.5	0.46 ^c	Table 4
38	1.5	0.12	Table 4
42	0.4	0.14 ^c	Table 4
44	0.6	0.24	Table 4
45	1	0.31 ^c	Table 4
46	0.7	0.38 ^c	Table 4
53	0.7	0.39 ^c	Table 4

^aMeasurements are reported as the mean of two or more independent experiments, each conducted in duplicate. ^bEvaluated via displacement of **S1**. ^cEvaluated via displacement of **S2**.

Solubility and Permeability Measurements. Caco-2 parameters were determined as described previously.⁶ Aqueous solubility was determined from 1 mg/mL of solid compound dispensed into aqueous McIlvaine buffer (pH 4.5 or 6.8), or dissolved in acetonitrile/water (1:1 v/v) as reference. Dissolved concentrations were determined with an Agilent 1200 HPLC/DAD-UV system.

Table S2. In Vitro Solubility and Permeability Measurements for Select Compounds.

Compd	HT sol ($\mu\text{g/mL}$) pH: 4.5 ^a	HT sol ($\mu\text{g/mL}$) pH: 6.8 ^a	$P_{\text{app A}\rightarrow\text{B}}$ (cm/s) ^b	$P_{\text{app B}\rightarrow\text{A}}$ (cm/s) ^b	efflux (B \rightarrow A/A \rightarrow B)
47	>130	39	--	--	--
55	100	94	--	--	--
58	71	<1	--	--	--
59	<1	<1	--	--	--
60	91	3	2.18×10^{-06}	3.02×10^{-05}	13.9
61	76	70	6.36×10^{-07}	2.51×10^{-05}	39.5
62	95	<1	$<1.96 \times 10^{-06}$	2.46×10^{-05}	>12.6
63	89	69	$<9.99 \times 10^{-07}$	9.35×10^{-06}	>9.4
64	>100	>110	1.76×10^{-06}	3.00×10^{-05}	17.1
65	82	<1	$<8.57 \times 10^{-07}$	8.76×10^{-06}	>10.2

^aMeasurements are reported as the result of a single experiment. ^bMeasurements are reported as the mean of two independent experiments.

Cell Culture. HeLa (ATCC CCL-2) and NCI-H727 (ATCC CRL-5815) cells were obtained from the ATCC and cultured in DMEM or RPMI supplemented with 10% (v/v) FBS, where appropriate. Cell lines were authenticated by STR profiling using PowerPlex 16HS technology and were tested negative for mycoplasma using the eMYCO Plus kit PCR test in October 2017 (Genetica DNA Laboratories). After thawing from liquid N₂, cells were passaged at least twice before use in experiments, and passaged for a maximum of 25 times.

Active RAS-GTP Pull-Down and Western Blotting. Cells were seeded to reach 70% confluency after 24 h incubation, and subsequently treated as indicated. Lysates were resolved by SDS-PAGE and transferred onto Immobilon-FL PVDF membranes (Millipore). Membranes were probed with primary antibodies as indicated, incubated with labeled secondary antibody, and scanned using an Odyssey imager (LI-COR). Levels of RAS-GTP were determined using an active RAS pull-down and detection kit according to the manufacturer's instructions (Thermo Scientific #16117). Total RAS and α -tubulin were included as input loading controls for the RAF1-RBD pull-down. ERK1/2 lysates were prepared separately using 1X LI-COR Protein Loading Buffer with 10 mM DTT. Primary antibodies used for western blotting—pan-RAS (KRAS, NRAS and HRAS isoforms; #3339), ERK1/2 (#9102), pERK1/2^{T202/Y204} (#9106), and α -tubulin (#3873)—were all purchased from Cell Signaling. EGF was purchased from R&D Systems.

In-Cell Western. Cells were seeded in a 384-well, black-walled, μ -clear bottom plate (#781091, Greiner Bio-One) to reach 90% confluency after 24 h incubation. Cells were treated with a 2-fold serial dilution of a given compound between 1.5 and 100 μ M or vehicle control (DMSO) alone for 30 min. In addition, cells were treated with either 1 μ M MEK inhibitor trametinib⁷ for 30 min (negative control), or 50 ng/mL EGF for 5 min (positive control). After treatment, cells were fixed with 4% (v/v) formaldehyde solution (#F1635, Sigma Aldrich) for 10 min at room temperature. Following fixation, cells were permeabilized with PBS 0.1% (v/v) Triton X-100 for 5 min, washed four times with PBS 0.1% (v/v) Triton X-100, and then incubated in Odyssey blocking buffer (LI-COR) for 1 h. Cells were probed overnight at 4 °C with primary antibodies directed towards ERK1/2 (#4696) and pERK1/2^{T202/Y204} (#4370) that were both purchased from Cell Signaling. The appropriate antibody staining negative controls were also included on each plate. Next, each plate was washed five times in PBS 0.1% (v/v) TWEEN20, and subsequently probed with labeled secondary antibodies, goat α -mouse (700 channel) and goat α -rabbit (800 channel), for 1 h at room temperature. Plates were washed five times with PBS 0.1% (v/v) TWEEN20 and then each plate was read using the Odyssey Imaging System (LI-COR). The intensity of each color channel was quantified using LI-COR Application software (V 3.0.30). The pERK1/2^{T202/Y204} signal was normalized to the total ERK1/2 signal in each well, and then each well was normalized to the DMSO control. GraphPad Prism software (V 6.0d) was used to calculate EC₅₀ values for each compound.

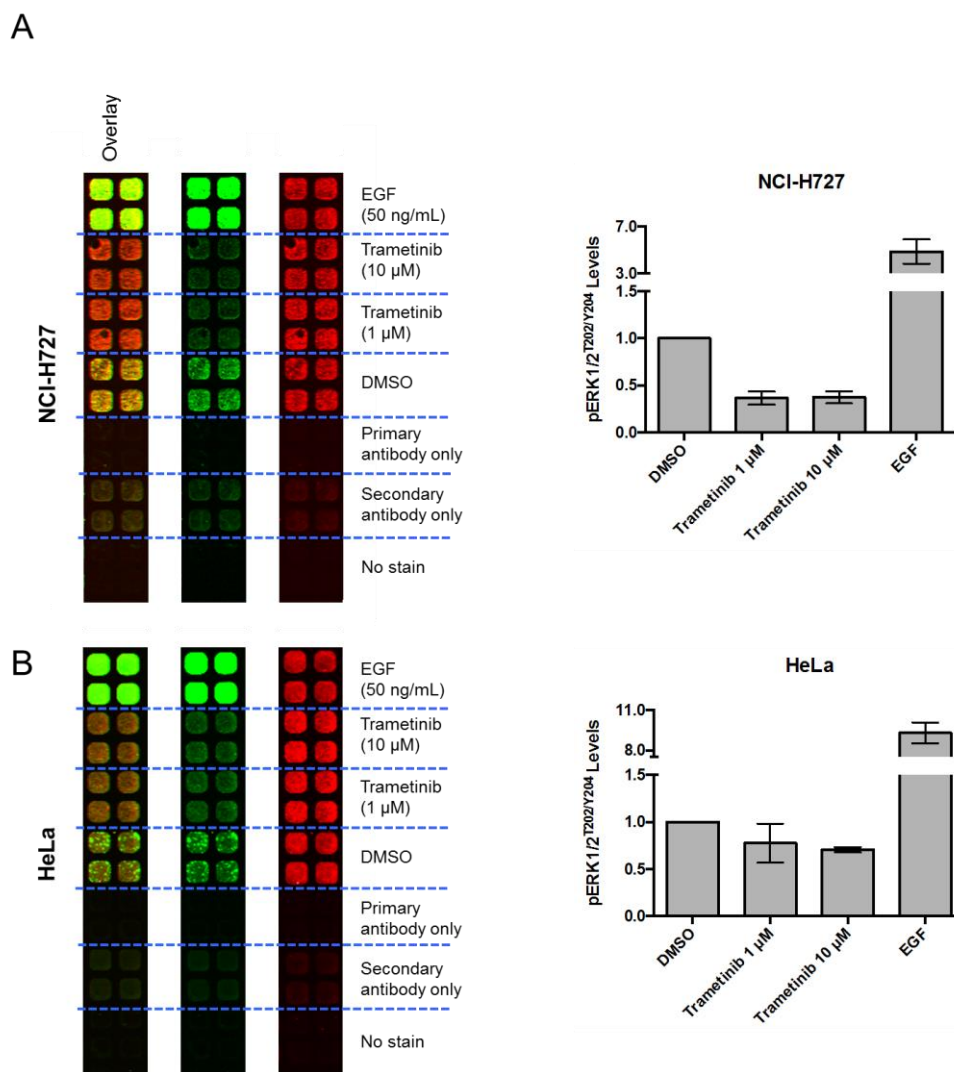
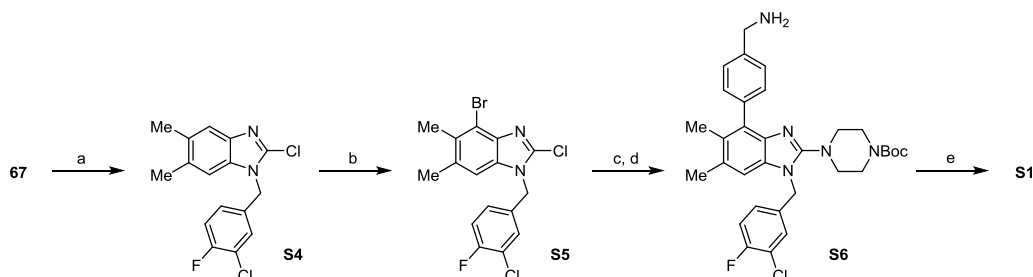


Figure S4. In-Cell Western analysis in (A) NCI-H727 cells and (B) HeLa cells. (LEFT) Representative ERK1/2 staining in response to treatment with the vehicle control (DMSO), 1 μM and 10 μM trametinib and EGF (50 ng/mL) controls. All compound treatments were for 30 min, except EGF, which was for 5 min. Green represents pERK1/2^{T202/Y204} levels and red represents total ERK1/2 levels. Primary, secondary, and no stain antibody controls were also included. (RIGHT) Quantification of pERK1/2^{T202/Y204} levels after treatment with vehicle control DMSO, negative control trametinib and positive control EGF. A broken scale on the y axis is used to visualize differences between the data in the set. Levels of pERK1/2^{T202/Y204} were normalized to total ERK1/2 levels for each well, and then normalized to the DMSO control on each plate. Data are the mean of four individual repeats. Error bars show standard deviation.

Chemistry Experimental Details

Syntheses of FPA Probes.

Scheme S1. Synthesis of FPA Probe S1.^a



^aReaction conditions: (a) 3-chloro-4-fluorobenzyl bromide, K₂CO₃, DMF, rt. (b) NBS, NMP, rt. (c) *tert*-butyl piperazine-1-carboxylate, *i*-Pr₂NEt, NMP, 150 °C in microwave. (d) (4-(aminomethyl)phenyl)boronic acid HCl, PdCl₂dppf·CH₂Cl₂, K₂CO₃, DMF/EtOH (4:1 v/v), 100 °C. (e) 5-carboxyfluorescein succinimidyl ester, DMAP, CH₂Cl₂/DMF, rt; then TFA.

2-Chloro-1-(3-chloro-4-fluorobenzyl)-5,6-dimethyl-1H-benzo[d]imidazole (S4). A mixture of 67 (200 mg, 1.1 mmol), 3-chloro-4-fluorobenzyl bromide (0.27 mg, 1.2 mmol), and K₂CO₃ (0.19 mg, 1.4 mmol) in DMF (3.7 mL) was stirred at rt for 16 h. The mixture was diluted with EtOAc, poured into a 50% sat. brine solution, and extracted with EtOAc (3x). The combined organics were washed with a 50% sat. brine solution, a sat. brine solution, dried (Na₂SO₄), and concentrated under reduced pressure. The crude residue was purified by silica gel chromatography to provide 348 mg of the title compound as a light yellow solid (98% yield). ¹H NMR (400 MHz, CD₃OD): δ 7.39 (s, 1H), 7.34 (dd, *J* = 6.9, 2.2 Hz, 1H), 7.25 (s, 1H), 7.21 (t, *J* = 8.7 Hz, 1H), 7.12 (ddd, *J* = 8.7, 4.5, 2.2 Hz, 1H), 5.46 (s, 2H), 2.36 (s, 6H). MS (ESI) *m/z* = 322.90 [M+H]⁺.

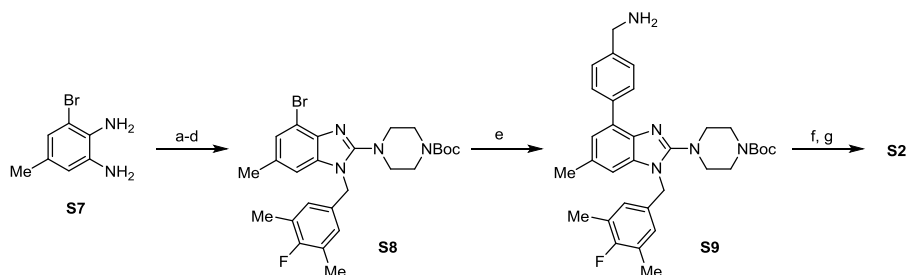
***tert*-Butyl 4-(4-bromo-1-(3-chloro-4-fluorobenzyl)-5,6-dimethyl-1H-benzo[d]imidazol-2-yl)piperazine-1-carboxylate (S5).** NBS (700 mg, 3.94 mmol) was added to a solution of S4 (1.06 g, 3.28 mmol) in NMP (17 mL) at 0 °C under an atmosphere of N₂. The cooling bath was removed, and the stirred reaction mixture was allowed to warm to rt. After 14 h, additional NBS (700 mg, 3.94 mmol) was added. After 26 h, the reaction mixture was diluted with 50% aq. NaHCO₃ and extracted with EtOAc (3x). The organic layers were combined, washed with H₂O, brine, dried (Na₂SO₄), and concentrated under reduced pressure. The crude residue was purified by silica gel chromatography to provide 463 mg of the title compound (35% yield). ¹H NMR (400 MHz, CDCl₃): δ 7.20 (dd, *J* = 6.7, 2.3 Hz, 1H), 7.09 (t, *J* = 8.6 Hz, 1H), 6.98 (ddd, *J* = 8.6, 4.4, 2.3 Hz, 1H), 6.91 (s, 1H), 5.27 (s, 2H), 2.46 (s, 3H), 2.39 (s, 3H). MS (ESI) *m/z* = 403.0 [M+H]⁺.

***tert*-Butyl 4-(4-(4-(aminomethyl)phenyl)-1-(3-chloro-4-fluorobenzyl)-5,6-dimethyl-1H-benzo[d]imidazol-2-yl)piperazine-1-carboxylate (S6).** A mixture of S5 (463 mg, 1.15 mmol), *N*-Boc-piperazine (1.72 g, 9.2 mmol), *i*-Pr₂NEt (0.401 mL, 298 mg, 2.3 mmol), and NMP (0.58 mL) was heated to 150 °C for 2 h in a microwave reactor. The reaction mixture was cooled to rt and then diluted with 50% aq. ammonium chloride and extracted with CH₂Cl₂ (3x). The organic layers were combined, washed with brine, dried (Na₂SO₄), and concentrated under reduced pressure. The residue was purified by silica gel chromatography to provide 462 mg of *tert*-butyl 4-(4-bromo-1-(3-chloro-4-fluorobenzyl)-5,6-dimethyl-1H-benzo[d]imidazol-2-yl)piperazine-1-carboxylate (73% yield). ¹H NMR (400 MHz, CDCl₃): δ 7.20 (dd, *J* = 6.7, 2.2 Hz, 1H), 7.12 (t, *J* = 8.6 Hz, 1H), 6.96 (ddd, *J* = 8.6, 4.3, 2.3 Hz, 1H), 6.73 (s, 1H), 5.13 (s, 2H), 3.55 (dd, *J* = 6.8, 4.8 Hz, 4H), 3.29 (br s, 4H), 2.44 (s, 3H), 2.35 (s, 3H), 1.46 (s, 9H). MS (ESI) *m/z* = 553.2 [M+H]⁺. A mixture of *tert*-butyl 4-(4-bromo-1-(3-chloro-4-fluorobenzyl)-5,6-dimethyl-1H-benzo[d]imidazol-2-yl)piperazine-1-carboxylate (361 mg, 0.90 mmol), (4-(aminomethyl)phenyl)boronic acid HCl (210 mg, 1.12 mmol), PdCl₂(dppf)·CH₂Cl₂ (65.7 mg, 0.0898 mmol), and K₂CO₃ (372 mg, 2.69 mmol) was charged with degassed DMF/EtOH (4:1 v/v, 3.0 mL) and heated to 100 °C under Ar(g). Upon complete consumption of the starting material,

as indicated by LC-MS, the reaction mixture was cooled to rt, diluted with 50% aq. ammonium chloride (60 mL), and extracted with EtOAc (3x). The organic layers were combined, washed with brine, dried (Na₂SO₄), and concentrated under reduced pressure. The residue was purified by silica gel chromatography to provide 192 mg of the title compound (37% yield). ¹H NMR (400 MHz, CD₃OD): δ 7.48 (d, *J* = 8.0 Hz, 2H), 7.36–7.32 (comp, 3H), 7.21 (t, *J* = 8.7 Hz, 1H), 7.11 (ddd, *J* = 8.7, 4.4, 2.1 Hz, 1H), 7.05 (s, 1H), 5.31 (s, 2H), 4.00 (s, 2H), 3.52–3.49 (br m, 4H), 3.07–3.05 (br m, 4H), 2.36 (s, 3H), 2.09 (s, 3H), 1.45 (s, 9H). MS (ESI) *m/z* = 578.1 [M+H]⁺.

4-((4-(1-(3-Chloro-4-fluorobenzyl)-5,6-dimethyl-2-(piperazin-1-yl)-1*H*-benzo[*d*]imidazol-4-yl)benzyl)carbamoyl)-2-(6-hydroxy-3-oxo-3*H*-xanthen-9-yl)benzoic acid (S1 as TFA salt). A single drop of DMF was added to a mixture of **S6** (8.0 mg, 0.014 mmol), 5-carboxyfluorescein succinimidyl ester (6.5 mg, 0.014 mmol), and DMAP (0.2 mg) in CH₂Cl₂ (0.5 mL). After 2 h at rt, TFA (0.5 mL) was added to the reaction mixture. After another 2 h at rt, the reaction mixture was concentrated and purified by reversed-phase HPLC. Pure fractions were concentrated under a warm stream of air to afford 2 mg of the title compound as the corresponding TFA salt. MS (ESI) *m/z* = 836.2 [M+H]⁺, 418.7 [M/2+H]⁺.

Scheme S2. Synthesis of FPA Probe **S2**.^a



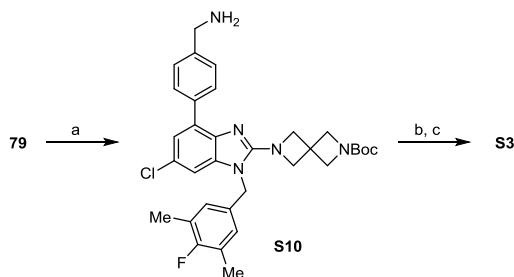
^aReaction conditions: (a) CDI, DMAP, CH₂Cl₂, rt. (b) POCl₃, 100 °C. (c) 4-fluoro-3,5-dimethylbenzyl bromide, K₂CO₃, DMF, rt. (d) *tert*-butyl piperazine-1-carboxylate, *i*-Pr₂NEt, NMP, 150 °C. (e) (4-(aminomethyl)phenyl)boronic acid HCl, Pd(OAc)₂, PCy₃·HBF₄, K₃PO₄, DME/H₂O (5:2 v/v), 80 °C. (f) FITC isomer 1, *i*-Pr₂NEt, DMF, rt. (g) TFA, CH₂Cl₂, rt.

***tert*-Butyl 4-(4-bromo-1-(4-fluoro-3,5-dimethylbenzyl)-6-methyl-1*H*-benzo[*d*]imidazol-2-yl)piperazine-1-carboxylate (S8).** Synthesized in analogous fashion to the preparation of **77** from **S7** in 47% yield over 4 steps. ¹H NMR (400 MHz, CDCl₃): δ 7.21 (d, *J* = 0.8 Hz, 1H), 6.75–6.73 (comp, 3H), 5.07 (s, 2H), 3.52 (dd, *J* = 6.8, 4.9 Hz, 4H), 3.22 (dd, *J* = 5.2, 3.6 Hz, 4H), 2.36 (s, 3H), 2.20 (d, *J* = 2.1 Hz, 6H), 1.46 (s, 9H). MS (ESI) *m/z* = 533.2 [M+H]⁺.

***tert*-Butyl 4-(4-(4-(aminomethyl)phenyl)-1-(4-fluoro-3,5-dimethylbenzyl)-6-methyl-1*H*-benzo[*d*]imidazol-2-yl)piperazine-1-carboxylate (S9).** A mixture of **S8** (500 mg, 0.941 mmol), (4-(aminomethyl)phenyl)boronic acid HCl (194 mg, 1.03 mmol), Pd(OAc)₂ (21.1 mg, 0.0941 mmol), tricyclohexylphosphine tetrafluoroborate (69.3 mg, 0.188 mmol) and K₃PO₄ (699 mg, 3.29 mmol) was charged with degassed DME/H₂O (5:2 v/v, 3.0 mL) and heated to 80 °C. After 6 h, more (4-(aminomethyl)phenyl)boronic acid HCl (194 mg, 1.03 mmol) was added. After an additional 16 h, the reaction mixture was allowed to cool to rt and partitioned between CH₂Cl₂ (50 mL) and 50% aq. ammonium chloride (50 mL). The layers were separated and the aqueous phase was extracted with CH₂Cl₂ (3x). The organic layers were combined, washed with sat. aq. NaHCO₃, brine, dried (Na₂SO₄), and concentrated under reduced pressure. The residue was purified by silica gel chromatography to provide 243 mg of the title compound (46% yield). ¹H NMR (400 MHz, CD₃OD): δ 7.91 (d, *J* = 7.9 Hz, 2H), 7.44 (d, *J* = 7.9 Hz, 2H), 7.15 (s, 1H), 6.95 (s, 1H), 6.87 (s, 1H), 6.86 (s, 1H), 5.24 (s, 2H), 3.90 (s, 2H), 3.54 (br s, 4H), 3.17–3.15 (br m, 4H), 2.43 (s, 3H), 2.19 (s, 6H), 1.46 (s, 9H). MS (ESI) *m/z* = 558.4 [M+H]⁺.

5-(3-(4-(1-(4-Fluoro-3,5-dimethylbenzyl)-6-methyl-2-(piperazin-1-yl)-1H-benzo[d]imidazol-4-yl)benzyl)thioureido)-2-(6-hydroxy-3-oxo-3H-xanthen-9-yl)benzoic acid (S2 as TFA salt). A mixture of **S9** (16 mg, 0.028 mmol) and fluorescein-5-isothiocyanate (isomer 1, 10 mg, 0.026 mmol) in DMF (0.5 mL) was charged with *i*-Pr₂NEt (7.0 mg, 9.0 μL, 0.051 mmol) and stirred at rt for 16 h. The reaction mixture was concentrated and redissolved in a 2:1 CH₂Cl₂/TFA solution (1.5 mL). After 4 h, the reaction mixture was concentrated and purified by reversed-phase preparative HPLC. The pure fractions were concentrated under a stream of warm air to afford 13 mg of the title compound as a TFA salt. MS (ESI) *m/z* = 846.9 [M+H]⁺, 424.0 [M/2+H]⁺.

Scheme S3. Synthesis of FPA Probe **S3**.^a



^aReaction conditions: (a) (4-(aminomethyl)phenyl)boronic acid HCl, PdCl₂dppf·CH₂Cl₂, Cs₂CO₃, dioxane, 80 °C. (b) FITC isomer 1, *i*-Pr₂NEt, DMF, rt. (c) TFA, CH₂Cl₂, rt.

5-(3-(4-(6-Chloro-1-(4-fluoro-3,5-dimethylbenzyl)-2-(2,6-diazaspiro[3.3]heptan-2-yl)-1H-benzo[d]imidazol-4-yl)benzyl)thioureido)-2-(6-hydroxy-3-oxo-3H-xanthen-9-yl)benzoic acid (S3 as TFA salt). A mixture of **79** (50 mg, 0.089 mmol), (4-(aminomethyl)phenyl)boronic acid HCl (25 mg, 0.13 mmol), PdCl₂dppf·CH₂Cl₂ (7.2 mg, 0.009 mmol), and Cs₂CO₃ (116 mg, 0.355 mmol) was charged with degassed dioxane (1.0 mL) and heated to 80 °C. After 16 h the reaction mixture was allowed to cool to rt and partitioned between CH₂Cl₂ and 50% aq. ammonium chloride. The layers were separated and the aqueous phase was extracted with CH₂Cl₂ (3x). The organic layers were combined, washed with sat. aq. NaHCO₃, brine, dried (Na₂SO₄), and concentrated under reduced pressure. The crude residue was partially purified by silica gel chromatography to provide 50 mg of impure **S10**. MS (ESI) *m/z* = 589.9 [M+H]⁺. Impure **S10** (14 mg, 0.023 mmol) was added to a solution of fluorescein-5-isothiocyanate (isomer 1, 8 mg, 0.021 mmol) and *i*-Pr₂NEt (6.0 mg, 8.0 μL, 0.046 mmol) in DMF (0.5 mL). The mixture was stirred at rt for 16 h, concentrated under reduced pressure, and redissolved in a mixture of CH₂Cl₂ (2 mL) and TFA (1 mL). After 3 h, the reaction mixture was concentrated under reduced pressure and purified by reversed-phase preparative HPLC. Pure fractions were concentrated under a stream of warm air to afford 6 mg of the title compound as a TFA salt. MS (ESI) *m/z* = 878.7 [M+H]⁺, 440.0 [M/2+H]⁺.

Structural Biology Experimental Details

Protein Expression and Purification. Details regarding protein expression and purification have been reported previously.^{1,2,4}

Crystallization, X-ray Data Collection, Structure Solution, and Refinement. Details regarding X-ray crystallography have been reported previously.^{1,2,4} Individual refinement statistics for all new structures are given in Table S3.

Table S3. X-ray Data Collection and Refinement Statistics.			
HRAS ^{WT} :SOS1 ^{cat} :HRAS:GppNHp			
Complex	3	10	28
PDB Entry	6D5V	6D5M	6D5L
Data collection			
Space group	I 4 2 2	I 4 2 2	I 4 2 2
Cell dimensions			
<i>a</i> , <i>b</i> , <i>c</i> (Å)	182.82, 182.82, 177.87	183.13, 183.13, 178.33	183.76, 183.76, 178.44
α , β , γ (°)	90.00, 90.00, 90.00	90.00, 90.00, 90.00	90.00, 90.00, 90.00
Resolution (Å) ^a	32.32 – 2.04 (2.11 – 2.04)	33.41 – 2.08 (2.16 – 2.08)	48.69 – 1.70 (1.76 – 1.70)
<i>R</i> _{merge} ^b	12.2 (85.3)	11.5 (60.5)	9.8 (94.7)
<i>I</i> / σ <i>I</i>	22.62 (4.60)	25.07 (5.5)	24.25 (3.16)
Completeness (%)	100.00 (100.00)	100.00 (100.00)	100.00 (100.00)
Redundancy	18.3 (18.3)	15.0 (15.1)	11.6 (10.7)
Structure Refinement			
No. reflections	94986	90155	165740
<i>R</i> _{work} / <i>R</i> _{free}	16.69 / 18.74	17.47 / 19.42	15.98 / 17.64
<i>B</i> -factors			
Protein	25.90	23.08	20.55
Water	37.27	34.21	37.32
Ligand	23.00	17.40	24.04
R.m.s. deviations			
Bond lengths (Å)	0.008	0.009	0.007
Bond angles (°)	1.080	1.080	0.850

^aValues in parentheses describe the highest resolution shell.

^b $R_{\text{merge}} = \frac{\sum_{hkl} \sum_i |I_i(hkl) - \langle I(hkl) \rangle|}{\sum_{hkl} \sum_i I_i(hkl)}$, where $I_i(hkl)$ is the observed intensity and $\langle I(hkl) \rangle$ is the average intensity obtained from multiple observations of symmetry-related reflections.

Table S3 cont. X-ray Data Collection and Refinement Statistics.			
HRAS ^{WT} :SOS1 ^{cat} :HRAS ^{Y64A} :Gpp			
NHp Complex	29	38	43
PDB Entry	6D5J	6D5H	6D5G
Data collection			
Space group	I 4 2 2	I 4 2 2	I 4 2 2
Cell dimensions			
<i>a</i> , <i>b</i> , <i>c</i> (Å)	183.63, 183.63, 179.06	184.14, 184.14, 179.24	183.05, 183.05, 178.78
α , β , γ (°)	90.00, 90.00, 90.00	90.00, 90.00, 90.00	90.00, 90.00, 90.00

Resolution (Å) ^a	48.72 – 1.75 (1.81 – 1.75)	43.34 – 1.80 (1.86 – 1.80)	48.59 – 1.92 (1.99 – 1.92)
R_{merge}^b	9.3 (81.9)	14.0 (186.0)	11.6 (85.7)
$I / \sigma I$	26.88 (3.47)	19.36 (2.0)	27.82 (4.25)
Completeness (%)	100.00 (100.00)	100.0 (100.0)	100.00 (100.00)
Redundancy	12.2 (11.8)	16.5 (16.5)	16.6 (16.5)

Structure Refinement

No. reflections	151872	140848	114803
$R_{\text{work}} / R_{\text{free}}$	15.74 / 17.52	16.89 / 19.01	15.54 / 17.25
B-factors			
Protein	23.92	25.51	23.48
Water	39.87	38.39	36.95
Ligand	28.69	30.99	30.65
R.m.s. deviations			
Bond lengths (Å)	0.007	0.008	0.007
Bond angles (°)	1.170	1.040	0.890

^aValues in parentheses describe the highest resolution shell.

^b $R_{\text{merge}} = \sum_{hkl} \sum_i |I_i(hkl) - \langle I(hkl) \rangle| / \sum_{hkl} \sum_i I_i(hkl)$, where $I_i(hkl)$ is the observed intensity and $\langle I(hkl) \rangle$ is the average intensity obtained from multiple observations of symmetry-related reflections.

Table S3 cont. X-ray Data Collection and Refinement Statistics.

HRAS ^{WT} :SOS1 ^{cat} :HRAS ^{Y64A} :Gpp			
NHp Complex	47	58	65
PDB Entry	6D5E	6D59	6D56
Data collection			
Space group	I 4 2 2	I 4 2 2	I 4 2 2
Cell dimensions			
<i>a</i> , <i>b</i> , <i>c</i> (Å)	183.61, 183.61, 179.18	184.11, 184.11, 179.43	183.62, 183.62, 178.74
α , β , γ (°)	90.00, 90.00, 90.00	90.00, 90.00, 90.00	90.00, 90.00, 90.00
Resolution (Å) ^a	43.22 – 1.75 (1.81 – 1.75)	32.12 – 1.70 (1.76 – 1.70)	42.69 – 1.68 (1.74 – 1.68)
R_{merge}^b	11.6 (130.8)	10.5 (125.8)	8.8 (89.6)
$I / \sigma I$	24.19 (2.54)	21.71 (2.25)	28.74 (3.56)
Completeness (%)	100.00 (100.00)	100.00 (100.00)	100.00 (100.00)
Redundancy	16.3 (15.7)	12.2 (11.8)	12.2 (11.7)
Structure Refinement			
No. reflections	152495	166987	171937
$R_{\text{work}} / R_{\text{free}}$	15.95 / 17.35	15.70 / 17.30	15.94 / 17.07
B-factors			
Protein	26.80	24.09	23.80
Water	42.42	40.37	39.54
Ligand	34.17	27.94	33.62
R.m.s. deviations			
Bond lengths (Å)	0.013	0.007	0.007
Bond angles (°)	0.850	0.840	1.170

^aValues in parentheses describe the highest resolution shell.

${}^bR_{\text{merge}} = \sum_{hkl} \sum_i |I_i(hkl) - (I(hkl))| / \sum_{hkl} \sum_i I_i(hkl)$, where $I_i(hkl)$ is the observed intensity and $(I(hkl))$ is the average intensity obtained from multiple observations of symmetry-related reflections.

Table S3 cont. X-ray Data Collection and Refinement Statistics.	
HRAS ^{WT} :SOS1 ^{cat} :HRAS ^{Y64A} :GppNHp	
Complex	64
PDB Entry	6D55
Data collection	
Space group	I 4 2 2
Cell dimensions	
<i>a</i> , <i>b</i> , <i>c</i> (Å)	183.48, 183.48, 179.40
α , β , γ (°)	90.00, 90.00, 90.00
Resolution (Å) ^a	38.95 – 1.68 (1.74 – 1.68)
R_{merge} ^b	11.0 (94.8)
<i>I</i> / σI	21.86 (2.71)
Completeness (%)	100.00 (99.90)
Redundancy	11.7 (10.8)
Structure Refinement	
No. reflections	171623
R_{work} / R_{free}	15.57 / 17.79
<i>B</i> -factors	
Protein	23.10
Water	38.92
Ligand	26.63
R.m.s. deviations	
Bond lengths (Å)	0.017
Bond angles (°)	1.630

^aValues in parentheses describe the highest resolution shell.

^b $R_{\text{merge}} = \sum_{hkl} \sum_i |I_i(hkl) - (I(hkl))| / \sum_{hkl} \sum_i I_i(hkl)$, where $I_i(hkl)$ is the observed intensity and $(I(hkl))$ is the average intensity obtained from multiple observations of symmetry-related reflections.

References

- (1) Burns, M. C.; Sun, Q.; Daniels, R. N.; Camper, D.; Kennedy, J. P.; Phan, J.; Olejniczak, E. T.; Lee, T.; Waterson, A. G.; Rossanese, O. W.; Fesik, S. W. Approach for Targeting Ras with Small Molecules That Activate SOS-Mediated Nucleotide Exchange. *Proc. Natl. Acad. Sci. U. S. A.* **2014**, *111* (9), 3401–3406.
- (2) Burns, M. C.; Howes, J. E.; Sun, Q.; Little, A. J.; Camper, D. V.; Abbott, J. R.; Phan, J.; Lee, T.; Waterson, A. G.; Rossanese, O. W.; Fesik, S. W. High-Throughput Screening Identifies Small Molecules That Bind to the RAS:SOS:RAS Complex and Perturb RAS Signaling. *Anal. Biochem.* **2018**, *548*, 44–52.
- (3) Abbott, J. R.; Hodges, T. R.; Daniels, R. N.; Patel, P. A.; Kennedy, J. P.; Howes, J. E.; Akan, D. T.; Burns, M. C.; Sai, J.; Sobolik, T.; Beesetty, Y.; Lee, T.; Rossanese, O. W.; Phan, J.; Waterson, A. G.; Fesik, S. W. Discovery of Aminopiperidine Indoles That Activate the Guanine Nucleotide Exchange Factor SOS1 and Modulate RAS Signaling. *J. Med. Chem.* **2018**, *61* (14), 6002–6017.
- (4) Sun, Q.; Burke, J. P.; Phan, J.; Burns, M. C.; Olejniczak, E. T.; Waterson, A. G.; Lee, T.; Rossanese, O. W.; Fesik, S. W. Discovery of Small Molecules That Bind to K-Ras and Inhibit Sos-Mediated Activation. *Angew. Chemie Int. Ed.* **2012**, *51* (25), 6140–6143.
- (5) Nikolovska-Coleska, Z.; Wang, R.; Fang, X.; Pan, H.; Tomita, Y.; Li, P.; Roller, P. P.; Krajewski, K.; Saito, N. G.; Stuckey, J. A.; Wang, S. Development and Optimization of a Binding Assay for the XIAP BIR3 Domain Using Fluorescence Polarization. *Anal. Biochem.* **2004**, *332* (2), 261–273.
- (6) Luippold, A. H.; Arnhold, T.; Jörg, W.; Krüger, B.; Süßmuth, R. D. Application of a Rapid and Integrated Analysis System (RIAS) as a High-Throughput Processing Tool for In Vitro ADME Samples by Liquid Chromatography/Tandem Mass Spectrometry. *J. Biomol. Screen.* **2011**, *16* (3), 370–377.
- (7) Abe, H.; Kikuchi, S.; Hayakawa, K.; Iida, T.; Nagahashi, N.; Maeda, K.; Sakamoto, J.; Matsumoto, N.; Miura, T.; Matsumura, K.; Seki, N.; Inaba, T.; Kawasaki, H.; Yamaguchi, T.; Kakefuda, R.; Nanayama, T.; Kurachi, H.; Hori, Y.; Yoshida, T.; Kakegawa, J.; Watanabe, Y.; Gilmartin, A. G.; Richter, M. C.; Moss, K. G.; Laquerre, S. G. Discovery of a Highly Potent and Selective MEK Inhibitor: GSK1120212 (JTP-74057 DMSO Solvate). *ACS Med. Chem. Lett.* **2011**, *2* (4), 320–324.